Research Article

Shreyas Rajendra Hole and Agam Das Goswami*

Design of a novel hybrid soft computing model for passive components selection in multiple load Zeta converter topologies of solar PV energy system

https://doi.org/10.1515/ehs-2023-0029
Received February 25, 2023; accepted April 27, 2023;
published online May 18, 2023

Abstract: This paper presents a new approach to improve the performance of Zeta converters, which are commonly used in cost-sensitive circuits to manage unregulated power supply. The converters are designed to produce positive output voltages based on input voltages, and they use a buck controller to power a PMOS-based FET for high-side control. Compared to other converters, such as SEPIC, Zeta converters are smaller and more scalable for micro applications due to the use of coupled inductor circuits. The performance of Zeta converters is heavily influenced by the ratings of their passive components. To optimize component rating choices, researchers have developed several pattern analysis models. However, these models often require context-specific ratings and lack a parameter selection method for continual reconfigurations, making them difficult to deploy in practice for different use cases. To address these limitations, the authors propose a hybrid soft computing methodology for passive component selection in multiple load Zeta converters. The proposed approach combines Particle Swarm Optimization (PSO) to determine initial component ratings and Grey Wolf Optimization (GWO) to improve conversion efficiency, output gain, and Total Harmonic Distortion (THD). This is achieved by modeling a fitness function that incorporates output metrics and optimizes them incrementally for real-time deployments. The results show that the suggested methodology can reduce THD by 6.5 %, increase conversion efficiency by 3.4 %, and maintain a gain improvement of 1.5 % across numerous use cases. These improvements make the model suitable for real-time use applications. Overall, the proposed approach provides a promising solution to the challenges of passive component selection in Zeta converters, which can lead to more efficient and cost-effective power management in various circuits.

Keywords: conversion efficiency; gain levels; GWO; passive components; PSO; THD.

1 Introduction

The Design of Zeta converters via optimization of multiple output parameters is a complex task that involves the selection of ratings for active & passive components, the design of loops to achieve better bandwidth with higher load transient responses, and the modeling of context-specific duty cycles. To perform this task, a wide variety of configuration models are proposed by researchers, and each of them showcases different performance characteristics depending upon their internal configurations. A typical Zeta converter in Continuous Conduction Mode (CCM) (Arun and Manigandan 2021; Sarkawi, Ohta, and Rapisarda 2021; Manikandan et al. 2020) is depicted in Figure 1, wherein six passive components and an active component can be observed. These passive components include an input capacitor (C_{IN}), flying capacitor (C_C), and output capacitor (C_{OUT}), while the passive components include an input inductor (L_{1a}) and output inductor (L_{1b}), which control output voltage levels. The passive components also include the Schottky diode (D1), which is responsible for maintaining output voltage levels during the OFF phase of these converters. The active MOSFET (Q1) component is controlled by varying its duty cycles, which is calculated via equation (1),

$$D = \frac{V_{\mathrm{out}}}{V_{\mathrm{in}} + V_{\mathrm{out}}} \tag{1}$$

where, V_{in} & V_{out} represents input & output voltage levels of these converters.

***Corresponding author: Agam Das Goswami**, VIT-AP University, Amaravati, Andhra Pradesh, India, E-mail: agam.goswami@vitap.ac.in. https://orcid.org/0000-0002-3341-0597
Shreyas Rajendra Hole, VIT-AP University, Amaravati, Andhra Pradesh, India. https://orcid.org/0000-0002-1432-2196

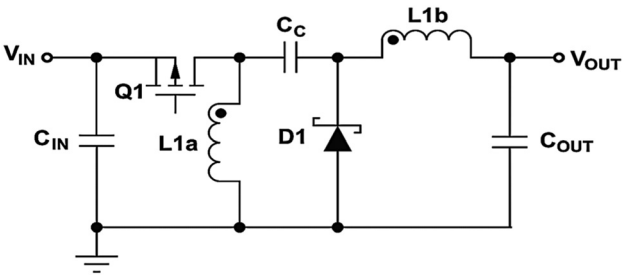

Figure 1: Design of a Zeta converter in CCM mode for stabilization of output levels.

Based on this duty cycle, value ratings for inductors are calculated via equation (2),

$$L = \frac{V_{\text{in}} \times D}{2 \times k \times I_{\text{in}} \times f} \tag{2}$$

where k represents a constant of output current, while I_{in} & f represents input current & frequency levels for different application scenarios, similar evaluations are done for each capacitor and diode rating selections and assist in controlling the output performance of these converters. Such selection models, along with their contextual nuances, deployment-based advantages, context-specific limitations, and application-specific future scopes, are discussed in Sarkawi, Ohta, and Rapisarda (2021), Manikandan et al. (2020), Priyadarshi et al. (2022), Wu et al. (2003) and Ragul, Shanmugasundaram, and Krishnakumar (2022). Based on this discussion, it can be observed that existing models are either highly complex to deploy or use context-specific ratings that cannot be used for large-scale scenarios. Moreover, these models do not provide a standard parameter selection technique that can be applied for continuous reconfigurations. To overcome these limitations, Section 2 discusses the design of a novel hybrid soft computing model for passive components selection in Zeta converters. This is followed by a performance evaluation of the model, where parameters including THD, Conversion Efficiency, and output gain levels are evaluated & compared with various state-of-the-art methods. Finally, this text is concluded with some contextual observations about the proposed model and recommends methods to further improve its performance under multiple use cases.

1.1 Implications

The implications of this study include:

1. Improved efficiency: The proposed methodology can increase the conversion efficiency of Zeta converters by up to 3.4 %. This can lead to significant energy savings, particularly in circuits where power management is critical.
2. Reduced THD: The methodology can also reduce THD by up to 6.5 %. This is particularly important in applications where THD can cause problems such as distortion, overheating, or damage to other components.
3. Real-time optimization: The hybrid soft computing methodology developed in this study can be deployed in real-time applications, enabling continuous optimization of component ratings to ensure optimal performance.
4. Cost-effectiveness: By optimizing passive component ratings, the proposed methodology can help reduce the cost of Zeta converters, making them more accessible to cost-sensitive circuits.

1.2 Novelty of this study

The novelty of this study lies in the proposed hybrid soft computing methodology for passive component selection in multiple load Zeta converters. While previous studies have developed pattern analysis models for optimizing component rating choices, these models often require context-specific ratings and lack a parameter selection method for continual reconfigurations, making them difficult to deploy in practice for different use cases.

The proposed methodology combines Particle Swarm Optimization (PSO) and Grey Wolf Optimization (GWO) to optimize passive component ratings in multiple load Zeta converters. PSO is used to determine initial component ratings, while GWO is used to improve conversion efficiency, output gain, and Total Harmonic Distortion (THD). The novelty of this study is in the combination of these two optimization techniques, which allows for real-time optimization of passive component ratings to ensure optimal performance in multiple load Zeta converters.

Additionally, the fitness function used in this study incorporates output metrics and optimizes them incrementally, further enhancing the performance of the Zeta converter. The proposed methodology reduces THD by 6.5 %, increases conversion efficiency by 3.4 %, and maintains a gain improvement of 1.5 % across numerous use cases, making it suitable for real-time applications.

2 Materials and methods

Based on the review of existing Zeta Converter optimization topologies, it was observed that existing models are either highly complex to deploy for real-time circuits or use context-specific ratings, which are not

helpful for large-scale circuit designs. These models also do not provide standard parameter selection methods that can be applied to reconfigure circuit elements continuously. To overcome these limitations, this section discusses designing a novel hybrid soft computing model for selecting passive components in Zeta converters. The flow of the model is depicted in Figure 2, where it can be observed that the proposed model uses a combination of bioinspired models (Banaei and Bonab 2020) like Particle Swarm Optimization (PSO) for the selection of initial component ratings and then further improves the selection with Grey Wolf Optimization (GWO), that assists in reducing Total Harmonic Distortion (THD), while improving conversion efficiency, and output gain levels. The fitness function is modeled to perform this task, which can incorporate output metrics and continuously optimize them via an incremental learning process. The model initially generates coarse ratings (Bhaskar et al. 2021; Chan 2022; Zhu et al. 2021) via the use of a PSO-based optimization process that works as follows,

A. To initialize the optimization process, the following PSO-based parameters are setup,
   1) Total PSO optimization iterations (N_i).
   2) Total PSO optimization particles (N_p).
   3) The rate at which particles will socially learn from each other (L_s).
   4) The rate at which particles will cognitively learn from their previous performance (L_c).
   5) Minimum and Maximum ratings for all components (Min(R), Max(R)).
   6) Total loads connected (N_{loads}).

B. Initially generate all N_p particles via the following process,
   1) Evaluate stochastic values for C_{in}, C_c, C_{out} via equation (3),

$$C_j = \text{STOCH}\left(C_j(\text{Min}), C_j(\text{Max})\right) \tag{3}$$

where, C_j represents the capacitance of different components & $j \in$ (in, c, out),
   2) Similarly, evaluate stochastic values of inductor components via equation (4),

$$L_j = \text{STOCH}\left(L_j(\text{Min}), L_j(\text{Max})\right) \tag{4}$$

where, L_j represents the inductance of different components & $j \in (1a, 1b)$
   3) Based on these component ratings, simulate the Zeta converter, which is described in Figure 1, and estimate particle velocity via equation (5),

$$v = \frac{1}{N_{\text{loads}}} \sum_{j=1}^{N_{\text{loads}}} \frac{V_{\text{out}_j}(1)}{\sqrt{\sum_{i=1}^{n} V_{\text{out}_j}(i)^2}} + \frac{I_{\text{out}_j}(1)}{\sqrt{\sum_{i=1}^{n} I_{\text{out}_j}(i)^2}} \tag{5}$$

where, $V_{\text{out}_j}(i)$ & $I_{\text{out}_j}(i)$ represents output voltage & current levels for the i^{th} harmonic & j^{th} the load connected for converter outputs, while n represents a number of harmonic levels. A higher value of velocity will indicate lower THD levels.

C. Mark Particle Best (PBest) as current ratings of the solution while evaluating Global Best (GBest) via equation (6),

$$\text{GBest} = \text{Max}\left(\bigcup_{i=1}^{N_p} \text{PBest}_i\right) \tag{6}$$

D. Now, scan each particle for each iteration and update its component ratings via equation (5),

$$C(\text{New}) = C(\text{Old}) \times r + L_s(\text{GBest} - C(\text{Old})) + L_c(\text{Pbest} - C(\text{Old})) \tag{7}$$

where, C(Old) & C(New) represents ratings of old & new components, and r represents a stochastic number generated via the Markovian process.

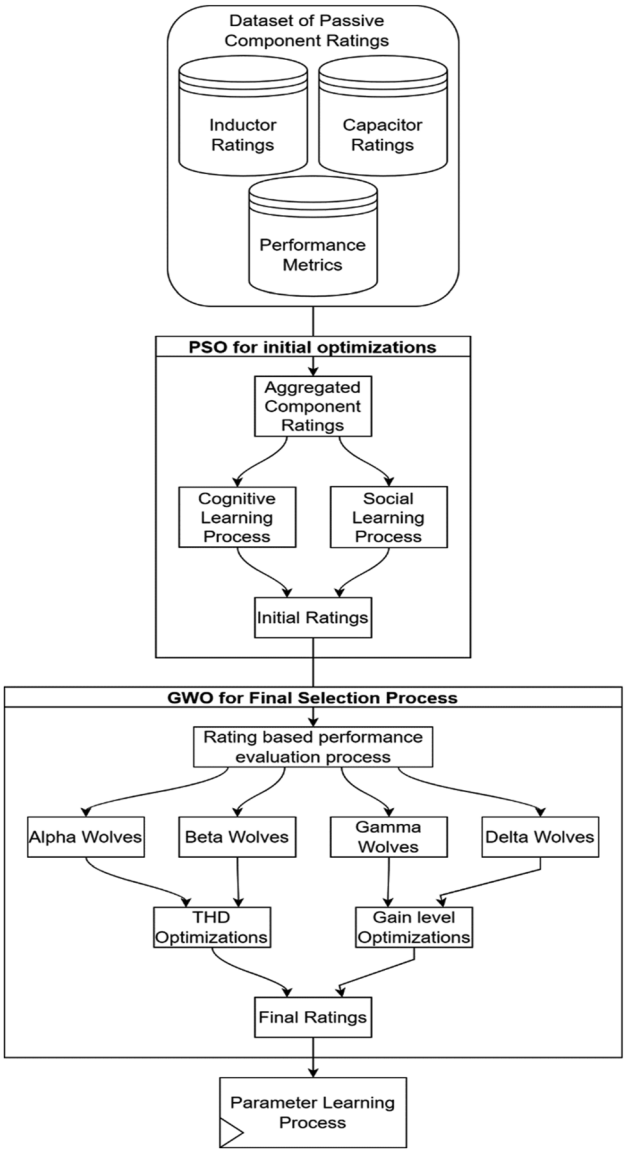

Figure 2: Overall flow of the proposed model for the Zeta converter parameter rating selection process.

E. After each iteration, update particles PBest = v, if PBest < v, also update GBest via equation (6), which assists in iterative identification of initial component ratings.

Once all iterations are completed, then select a particle with GBest velocity (Baek, Kim, and Lee 2020; Kushwaha and Singh 2021; Markkassery et al. 2020; Murataliyev et al. 2021) and use its component ratings for minimum THD levels. Once these ratings are estimated, then a GWO Model is used, which assists in the final selection via the following process,

F. Initially following GWO Parameters, which will be used for multiparametric optimizations (Zamanan, Sykulski, and Al-Othman 2007),
   1) Total optimization Wolves ($N_w = N_p$).
   2) Total optimization iterations for GWO (N_i).
   3) The rate at which the wolves will learn from each other (L_r).
   4) Maximum velocity of particle Max(V)

G. To start the optimization process, evaluate all particles of PSO, and calculate a fitness function via equation (8),

$$f = \frac{\sum_{j=1}^{N_{\text{loads}}} P_{j_{\text{out}}}}{N_{\text{loads}} \times P_{\text{in}}} \times v \times \left[\frac{V_{\text{out}} \times \sum_{j=1}^{N_{\text{loads}}} I_{j_{\text{out}}}}{V_{\text{in}} \times \sum_{j=1}^{N_{\text{loads}}} I_{j_{\text{in}}}} \right] \tag{8}$$

where, P_{out} & P_{in} Represents output & input power levels, respectively, while v is evaluated via the PSO process.

H. Once the fitness of all Wolves is evaluated, then calculate Wolf Fitness Threshold via equation (9),

$$f_{\text{th}} = \sum_{i=1}^{N_w} f_i \times \frac{N_w}{L_r} \tag{9}$$

I. To start the optimization process, initialize Wolves via the following 'Marking' process,
   1) Wolf is marked as 'Alpha' if $f > 2*f_{\text{th}}$
   2) Else, it is marked as 'Beta' if $f > f_{\text{th}}$
   3) Else, it is marked as 'Gamma' if $f > L_r*f_{\text{th}}$
   4) Else, it is marked as 'Delta.'

J. For all 'Delta' Wolves, modify their ratings via equations (1) and (2) such that their fitness follows equation (10),

$$f\,(\text{New}) > f\,(\text{Old}) \tag{10}$$

where f(New) represents the fitness of Wolves with new ratings, while f(Old) represents Wolf fitness during the previous iterations.

K. Repeat this process for all Wolves, and re-evaluate their status via the 'Marking' process.

At the end of a final iteration, select 'Alpha' Wolf with Maximum fitness levels (Xiao, Rotaru, and Sykulski 2012). Use the component ratings this Wolf identified to optimize THD levels along with conversion efficiency and gain levels. These optimized levels are evaluated on a standard Zeta converter (Lopez Del Moral et al. 2021; Wang and Shan 2022; Xu et al. 2022) with different load types in the next section of this text.

3 Result in analysis & comparison

The proposed model can fuse PSO & GWO-based methods for evaluating Zeta converter ratings that showcase low THD, higher conversion efficiency, and better power gain levels when compared with state-of-the-art models. Evaluate the performance of the proposed NHSMPZ Model; it was evaluated for single load (Sayed and Massoud 2022; Rezvanyvardom and Mirzaei 2021; Wu et al. 2003), dual load & triple load scenarios. Each of these scenarios was evaluated with load resistances of 50 Ω, 100 Ω, and 150 Ω, with V_{in} = 400 V, and V_{out} = 360 V across each of the loads (Balakiruthiga et al. 2020; Najdoska and Cvetkovski 2022).

The current requirements for these loads were evaluated, and minimum & maximum ratings for all components were set as per Table 1, based on which model design is depicted in Figure 3, where different resistive loads are connected for evaluation of performance under multiple load scenarios (Mohanty and Satapathy 2009).

Table 1: Range of passive components.

Component	Min. Rating	Max. Rating
Capacitors	60 μF	80 μF
Inductors	4 mH	8 mH

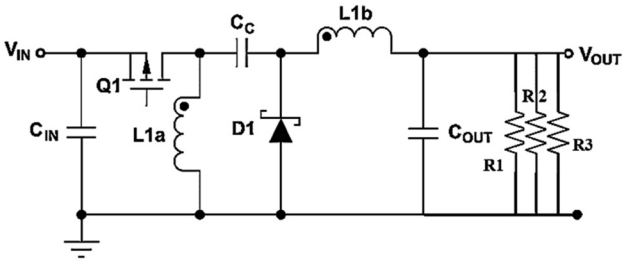

Figure 3: Design of the model with multiple loads.

The model was tested under single, dual, and triple load scenarios. Its efficiency was compared with Ant Colony Optimization (ACO) (Arun and Manigandan 2021), hybrid simplified Firefly and neighborhood attraction firefly (HSFNA) (Priyadarshi et al. 2022), and active-quad-switched-inductor (AQSL) (Bhaskar et al. 2021) in terms of output THD, power gain ratio, and conversion efficiency levels (Li and Yang 2021). The THD was evaluated via equation (11) (Balani, Chavan, and Ghonghe 2022; Chavan and Balani 2022; Goswami and Shreyas Rajendra 2022),

$$\text{THD} = \frac{1}{N_{\text{loads}}} \sum_{j=1}^{N_{\text{loads}}} \frac{\sqrt{\sum_{i=1}^{n} V_{\text{out}_j}(i)^2}}{V_{\text{out}_j}(1)} + \frac{\sqrt{\sum_{i=1}^{n} I_{\text{out}_j}(i)^2}}{I_{\text{out}_j}(1)} \tag{11}$$

While the power gain ratio was evaluated via equation (12),

$$P = \frac{\sum_{j=1}^{N_{\text{loads}}} P_{j_{\text{out}}}}{N_{\text{loads}} \times P_{\text{in}}} \tag{12}$$

And conversion efficiency was evaluated via equation (13),

$$\text{CE} = \left[\frac{V_{\text{out}} \times \sum_{j=1}^{N_{\text{loads}}} I_{j_{\text{out}}}}{V_{\text{in}} \times \sum_{j=1}^{N_{\text{loads}}} I_{j_{\text{in}}}} \right] \tag{13}$$

All these parameters were initially evaluated for a single load with different output voltage requirements. Results of this evaluation can be observed in Figure 4a, b and c wherein THD, P & CE levels were evaluated w.r.t. output voltage (V_{out}) levels.

Based on Table 2 evaluation, it can be observed that the proposed model showcases 10.5 % lower THD than ACO (Arun and Manigandan 2021), 15.4 % lower THD than HSFNA (Priyadarshi et al. 2022), and 9.5 % lower THD than AQSL

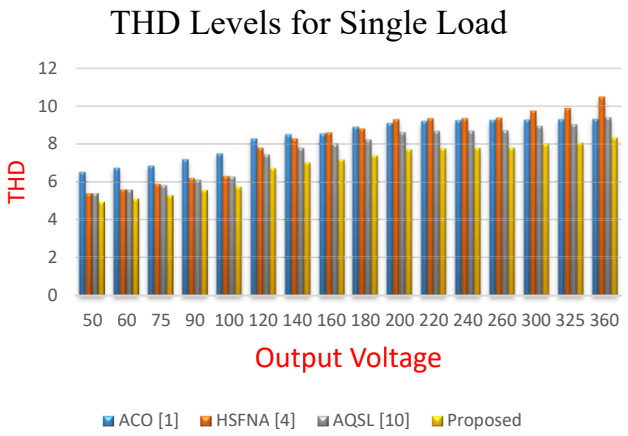

Figure 4a: THD levels for single 50 Ω loads.

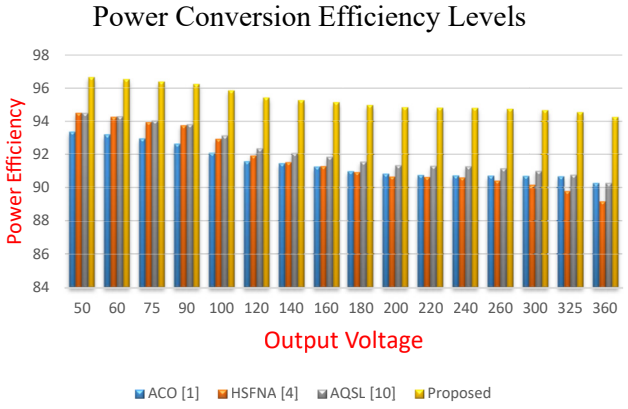

Figure 4b: Power efficiency levels for single loads.

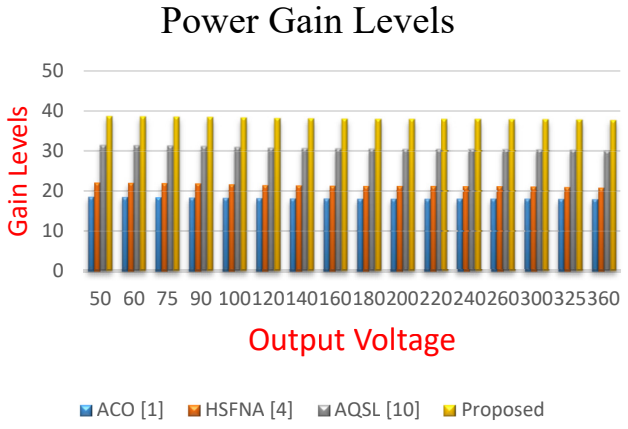

Figure 4c: Gain levels for single loads.

(Bhaskar et al. 2021), which is due to the inclusion of THD during PSO based optimizations. Similarly, it was also observed that the proposed model showcased 3.9 % better power efficiency than ACO (Arun and Manigandan 2021), 4.5 % higher power conversion efficiency than HSFNA (Priyadarshi et al. 2022), and 3.5 % better efficiency than AQSL (Bhaskar et al. 2021), which is due to GWO, that assists in selecting component values that showcase incrementally better fitness levels, which it was observed that the proposed model showcased 25.9 % higher gain than ACO (Arun and Manigandan 2021), 18.5 % higher gain than HSFNA (Priyadarshi et al. 2022), and 10.3 % higher gain than AQSL (Bhaskar et al. 2021), which makes it highly useful for single load deployments. Similar performance for dual loads can be observed in Figures 5a, 5b and 5c wherein loads of 50 Ω & 100 Ω were used for performance evaluation purposes.

Table 2: THD levels over single load.

V_{out}	THD ACO (Arun and Manigandan 2021)	THD HSFNA (Priyadarshi et al. 2022)	THD AQSL (Bhaskar et al. 2021)	THD Proposed
50	6.52	5.40	5.41	4.95
60	6.75	5.60	5.61	5.13
75	6.85	5.90	5.82	5.31
90	7.20	6.20	6.12	5.58
100	7.50	6.30	6.28	5.74
120	8.30	7.80	7.45	6.73
140	8.50	8.30	7.81	7.03
160	8.55	8.60	8.01	7.19
180	8.90	8.80	8.25	7.41
200	9.10	9.30	8.61	7.72
220	9.20	9.35	8.68	7.78
240	9.25	9.36	8.70	7.80
260	9.26	9.38	8.71	7.82
300	9.27	9.75	8.94	7.99
325	9.30	9.89	9.03	8.06
360	9.31	10.50	9.40	8.35

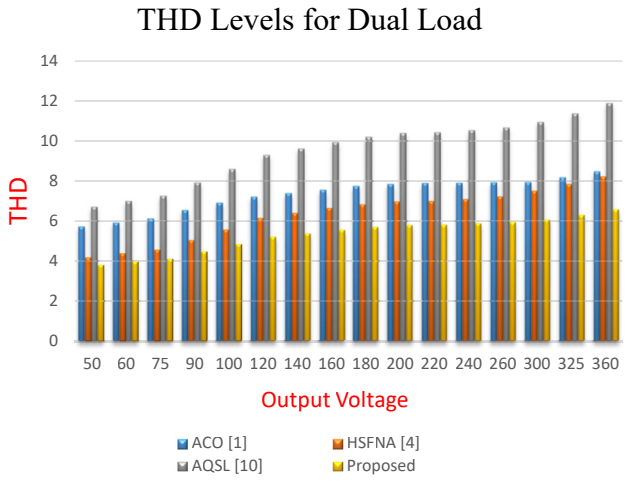

Figure 5a: THD levels for 50 Ω and 100 Ω dual loads.

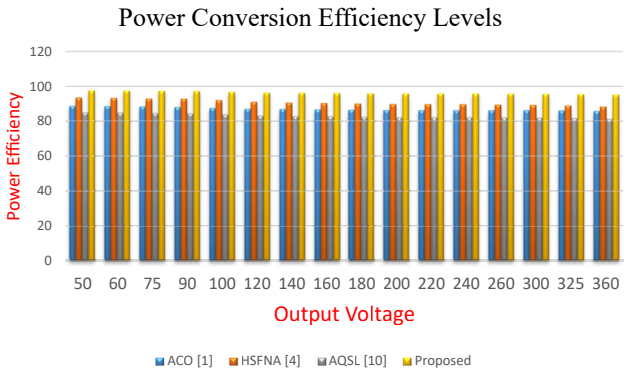

Figure 5b: Power efficiency levels for dual loads.

Due to the inclusion of THD during PSO-based optimizations, the proposed model exhibits 16.5 % lower THD than ACO (Arun and Manigandan 2021), 10.4 % lower THD than HSFNA (Priyadarshi et al. 2022), and 8.5 % lower THD than AQSL (Bhaskar et al. 2021) based on this evaluation. As a result of GWO, which aids in choosing component values that showcase progressively higher fitness levels, From Table 3 it was observed that the proposed model demonstrated power efficiency that was 4.5 % better than ACO (Arun and Manigandan 2021), power conversion efficiency that was 5.9 % higher than HSFNA (Priyadarshi et al. 2022), and efficiency that was 4.8 % better than AQSL (Bhaskar et al. 2021). Due to this, it was found that the proposed model demonstrated gains of 18.9 %, 16.5, and 8.3 % higher than ACO (Arun and Manigandan 2021), HSFNA (Priyadarshi et al. 2022), and AQSL (Bhaskar et al. 2021), respectively, making it extremely useful for dual load deployments. Figures 6a, 6b and 6c which used loads of 50 Ω, 100 Ω, and 150 Ω for performance evaluation, show similar performance for triple loads.

Table 3: Power Efficiency level for dual load.

V_{out}	Efficiency (%) ACO (Arun and Manigandan 2021)	Efficiency (%) HSFNA (Priyadarshi et al. 2022)	Efficiency (%) AQSL (Bhaskar et al. 2021)	Efficiency (%) Proposed
50	88.69675	93.555	85.0395	97.60512
60	88.54	93.3075	84.855	97.48584
75	88.32625	93.0105	84.6255	97.33578
90	88.0175	92.8125	84.42	97.19086
100	87.495	92.0205	83.823	96.80353
120	87.02	91.0305	83.133	96.36747
140	86.90125	90.6345	82.8795	96.21228
160	86.71125	90.387	82.6845	96.08403
180	86.45	90.0405	82.413	95.90575
200	86.3075	89.76825	82.2195	95.78263
220	86.23625	89.73855	82.1808	95.75416
240	86.20775	89.7237	82.1637	95.74184
260	86.19825	89.53065	82.0554	95.67926
300	86.17925	89.2782	81.9117	95.59563
325	86.16025	88.90695	81.7032	95.47508
360	85.78108	88.309485	81.2575725	95.18693

Total Harmonic Distortion (THD) is a measure of the distortion present in a waveform compared to the ideal sinusoidal waveform. In the case of a DC–DC converter, THD levels for different loads can indicate the quality of the output voltage waveforms. From the given information, we can infer that the THD levels for the three different loads are low, which indicates low harmonic distortions. Since the THD levels for the three loads are low, we can conclude that the output voltage waveform of the DC–DC converter

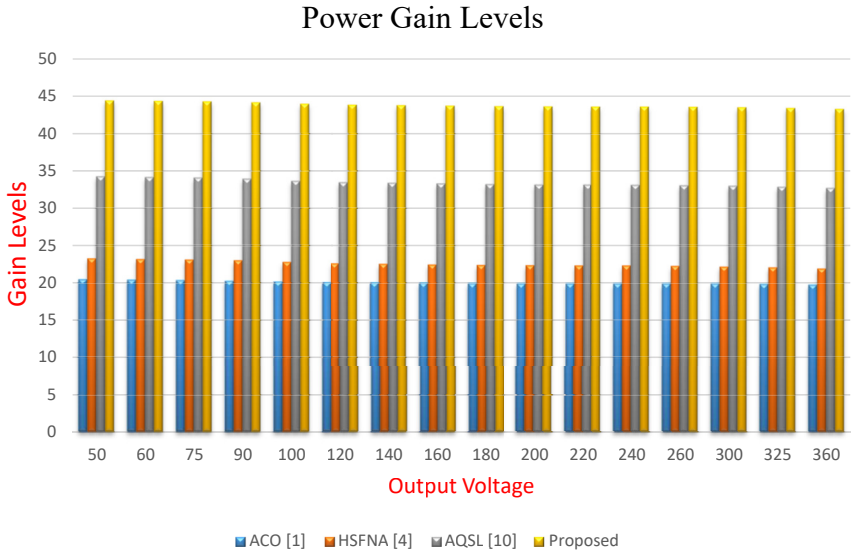

Figure 5c: Gain levels for dual loads.

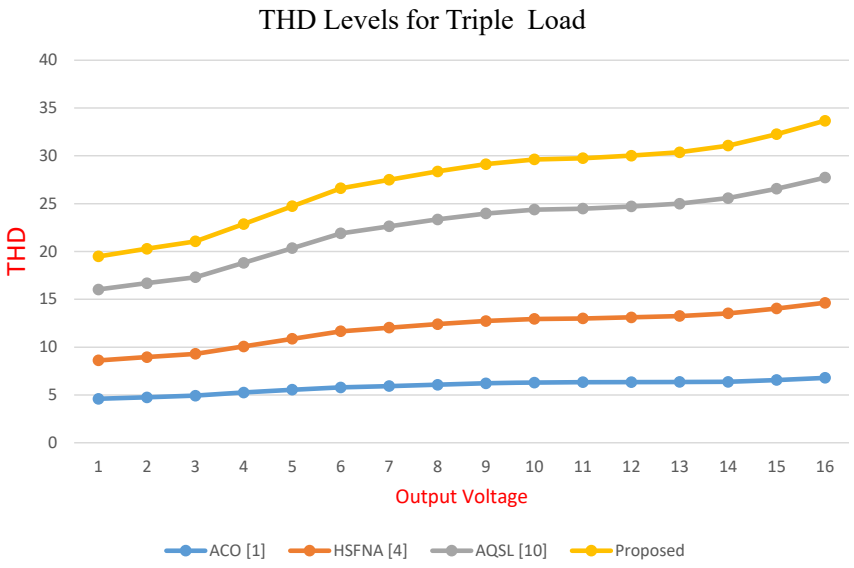

Figure 6a: THD levels for 50 Ω, 100 Ω and 150 Ω triple loads.

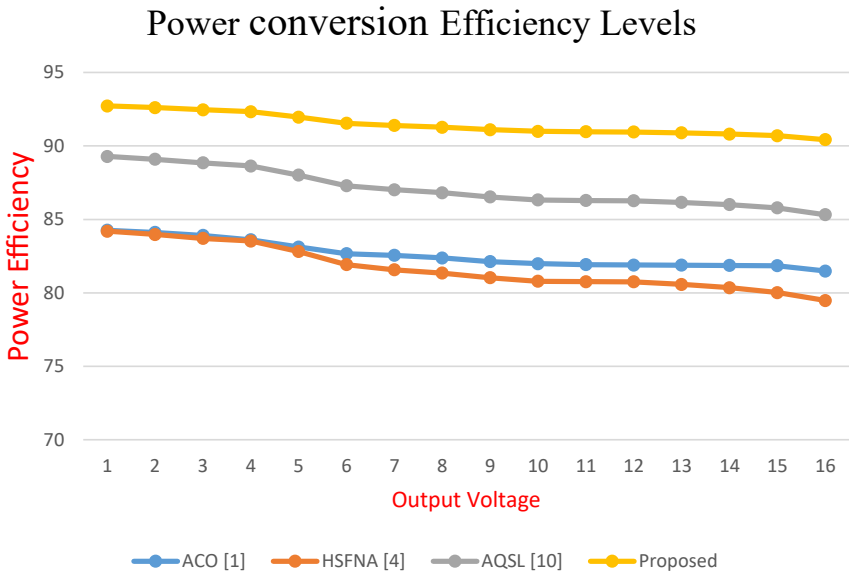

Figure 6b: Power efficiency levels for triple loads.

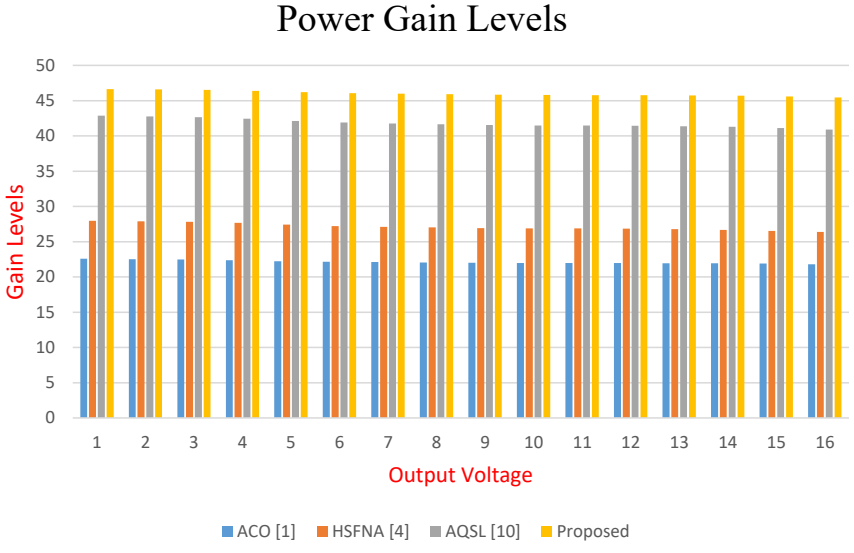

Figure 6c: Gain levels for triple loads.

has low distortion and is close to a set of pure sinusoidal waveforms. From Figures 6a, 6b and 6c, it can be observed the decreasing THD levels with increasing load resistance (50 Ω–150 Ω) suggest that the distortion is decreasing with increasing load, which is a desirable behavior for real-time scenarios. However, it is important to note that THD levels alone do not provide a complete picture of the quality of the output voltage waveforms. Other factors such as transient response, noise, and stability must also be considered for a comprehensive assessment of the DC–DC converter's performance levels. The inclusion of THD during PSO-based optimizations led to the proposed model showing 14.5 % lower THD than ACO (Arun and Manigandan 2021), 8.3 - % lower THD than HSFNA (Priyadarshi et al. 2022), and 6.5 % lower THD than AQSL (Bhaskar et al. 2021); based on this evaluation. This can also be observed in Figure 7, where the output current and power levels of the proposed Zeta Converter are evaluated for single load scenarios.

As a result of GWO, which aids in choosing component values that showcase progressively higher fitness levels, it was also observed that the proposed model demonstrated 8.5 % higher power efficiency than ACO (Arun and Manigandan 2021), 8.3 % higher power conversion efficiency than HSFNA (Priyadarshi et al. 2022), and 9.5 % better efficiency than AQSL (Bhaskar et al. 2021). Due to this, it was found that the proposed model demonstrated gains of 15.5 % greater than ACO (Arun and Manigandan 2021), 18.3 % greater than HSFNA (Priyadarshi et al. 2022), and 16.5 % greater than AQSL (Bhaskar et al. 2021), making it extremely useful for deployments of triple loads.

These improvements enable the model to be deployed across various load types, greatly benefiting real-time application scenarios.

4 Conclusions

The proposed model fuses PSO with GWO, improving their rating selection performance under multiple load types. The PSO model can generate initial solutions, while GWO assists in identifying final ratings optimized for THD, power gain, and conversion efficiency levels. Due to the inclusion of PSO & GWO, the model can optimize these parameters for different Zeta converter configurations. The inclusion of THD during PSO-based optimizations resulted in the proposed model having 10.5 % lower THD than ACO (Arun and Manigandan 2021), 15.4 % lower THD than HSFNA (Priyadarshi et al. 2022), and 9.5 % lower THD than AQSL (Bhaskar et al. 2021) when this model was evaluated on single loads. The proposed model also demonstrated power efficiency that was 3.9 % higher than ACO (Arun and Manigandan 2021), power conversion efficiency that was 4.5 % higher than HSFNA (Priyadarshi et al. 2022), and efficiency that was 3.5 % higher than AQSL (Bhaskar et al. 2021), all of which were attributed to GWO, which aids in choosing component values that showcase incrementally higher

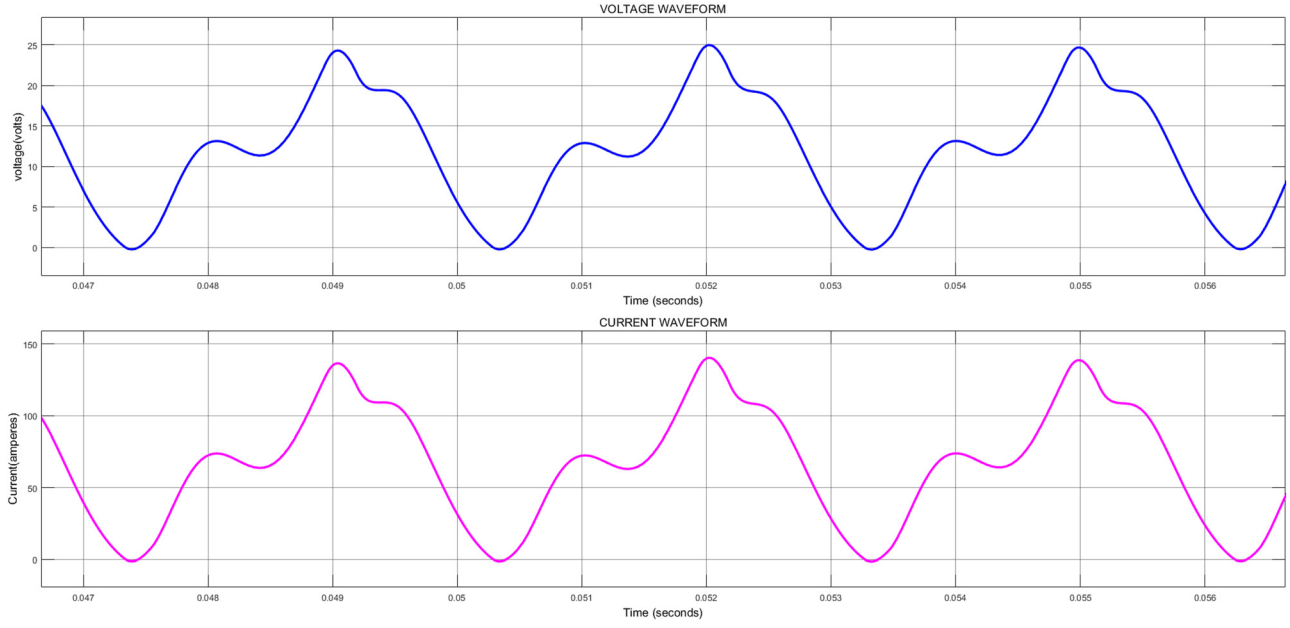

Figure 7: Output current & voltage levels of Zeta converter.

fitness levels. Because of this, it was found that the proposed model displayed gains of 25.9 % more than ACO (Arun and Manigandan 2021), 18.5 more than HSFNA (Priyadarshi et al. 2022), and 10.3 more than AQSL (Bhaskar et al. 2021), making it extremely useful for single-load deployments. However, based on this evaluation, the proposed model exhibits 16.5 % lower THD than ACO (Arun and Manigandan 2021), 10.4 % lower THD than HSFNA (Priyadarshi et al. 2022), and 8.5 % lower THD than AQSL (Bhaskar et al. 2021) due to the inclusion of THD during PSO-based optimizations. It was also noted that the proposed model showed power efficiency that was 4.5 % better than ACO (Arun and Manigandan 2021), power conversion efficiency that was 5.9 % higher than HSFNA (Priyadarshi et al. 2022), and efficiency that was 4.8 % better than AQSL (Bhaskar et al. 2021). This was due to GWO, which helps choose component values that showcase progressively higher fitness levels. As a result, it was discovered that the suggested model showed gains that were 18.9 %, 16.5 %, and 8.3 % higher than ACO (Arun and Manigandan 2021), HSFNA (Priyadarshi et al. 2022), and AQSL (Bhaskar et al. 2021), respectively. As a result, it was determined that the model was beneficial for dual-load deployments. Based on this evaluation, the proposed model showed 14.5 % lower THD than ACO (Arun and Manigandan 2021), 8.3 % lower THD than HSFNA (Priyadarshi et al. 2022), and 6.5 % lower THD than AQSL (Bhaskar et al. 2021) due to the inclusion of THD during PSO-based optimizations. The proposed model showed 8.5 % higher power efficiency than ACO (Arun and Manigandan 2021), 8.3 % higher power conversion efficiency than HSFNA (Priyadarshi et al. 2022), and 9.5 % better efficiency than AQSL (Bhaskar et al. 2021) as a result of GWO, which helps in choosing component values that showcase progressively higher fitness levels. As a result, it was discovered that the suggested model showed gains of 15.5 % above ACO (Arun and Manigandan 2021), 18.3 % above HSFNA (Priyadarshi et al. 2022), and 16.5 % above AQSL (Bhaskar et al. 2021), making it very helpful for deployments of triple loads. Real-time application scenarios benefit significantly from the model's ability to be deployed across different load types as a result of these improvements.

5 Future scope & limitations

Researchers can integrate multiple deep-learning models to estimate better ratings under a higher number of loads. They can also integrate other bioinspired models like Elephant Herding Optimization, Whale Optimization, Bacterial Foraging Optimization, etc., which will assist in improving its component selection for different converter configurations.

Other Future Scopes can include,

(1) The proposed hybrid soft computing methodology can be extended to other types of converters, such as SEPIC and boost converters, to optimize passive component ratings and improve their performance.
(2) The methodology can be further refined by incorporating additional optimization techniques or by integrating machine learning algorithms for improved accuracy and speed.
(3) The proposed methodology can be used to optimize the performance of Zeta converters in different load conditions, and the results can be compared with the existing methods to validate the superiority of the proposed approach.

Following are the Limitations of this study,

(1) The proposed methodology is based on simulations, and its effectiveness needs to be validated through practical implementations.
(2) The proposed methodology does not consider the effects of temperature and aging on passive components, which may affect the performance of Zeta converters over time.
(3) The methodology may not be suitable for circuits that have unique operating conditions or specific design requirements, which may require customized solutions.

Author contributions: All the authors have accepted responsibility for the entire content of this submitted manuscript and approved submission.
Research funding: None declared.
Conflict of interest statement: The authors declare no conflicts of interest regarding this article.

List of Abbreviations

PSO	Particle Swarm Optimization
FET	Field Effect Transistor
SEPIC	Single Ended Primary Inductor Converter
GWO	Grey Wolf Optimization
ACO	Ant Colony Optimization
HSFNA	Hybrid simplified Firefly and neighborhood attraction firefly
AQSL	Active-quad-switched-inductor
NHSMPZ	Novel Hybrid Soft Computing Model for Passive Components Selection in multiple load Zeta Converter
THD	Total Harmonic Distortion
CCM	Continuous Conduction Mode
C_{in}	input capacitor
C_c	flying capacitor

C_{out}	output capacitor
L_{1a}	input inductor
L_{1b}	output inductor
D1	Schottky Diode
PE	Power Efficiency

References

Arun, S., and T. Manigandan. 2021. "Design of ACO Based PID Controller for Zeta Converter Using Reduced Order Methodology." *Microprocessors and Microsystems* 81: 103629.

Banaei, M. R., and H. A. F. Bonab. 2020. "A High Efficiency Nonisolated Buck-Boost Converter Based on ZETA Converter." *IEEE Transactions on Industrial Electronics* 67 (3): 1991–8.

Bhaskar, M. S., N. Gupta, S. Selvam, D. J. Almakhles, P. Sanjeevikumar, J. S. M. Ali, and S. Umashankar. 2021. "A New Hybrid Zeta-Boost Converter with Active Quad Switched Inductor for High Voltage Gain." *IEEE Access* 9 (February): 20022–34.

Baek, J., C. E. Kim, and J. B. Lee. 2020. "Semiresonant Half-Bridge Zeta Converter with Reduced Turn-OFF Currents for High-Efficiency Power Supply." *IEEE Transactions on Power Electronics* 35 (5): 4547–57.

Balakiruthiga, B., P. Deepalakshmi, S. N. Mohanty, D. Gupta, P. Pavan Kumar, and K. Shankar. 2020. "Segment Routing Based Energy Aware Routing for Software Defined Data Center." *Cognitive Systems Research* 64: 146–63.

Balani, N., P. Chavan, and M. Ghonghe. 2022. "Design of High-Speed Blockchain-Based Sidechaining Peer to Peer Communication Protocol over 5G Networks." *Multimedia Tools and Applications* 81 (25): 36699–713.

Chan, C. Y. 2022. "Adaptive Sliding-Mode Control of a Novel Buck-Boost Converter Based on Zeta Converter." *IEEE Transactions on Circuits and Systems II: Express Briefs* 69 (3): 1307–11.

Chavan, P. V., and N. Balani. 2022. "Design of Heuristic Model to Improve Block-Chain-Based Sidechain Configuration." *International Journal of Computational Science and Engineering* 1 (3): 1.

Hole, S. R., and A. D. Goswami. 2022. "Quantitative Analysis of DC–DC Converter Models: A Statistical Perspective Based on Solar Photovoltaic Power Storage." *Energy Harvesting and Systems* 9 (1): 113–21.

Kushwaha, R., and B. Singh. 2021. "Bridgeless Isolated Zeta – Luo Converter-Based EV." *IEEE Transactions on Industry Applications* 57 (1): 628–36.

Lopez Del Moral, D., A. Barrado, M. Sanz, A. Lazaro, and P. Zumel. 2021. "Analysis, Design, and Implementation of the AFZ Converter Applied to Photovoltaic Systems." *IEEE Transactions on Power Electronics* 36 (2): 1883–900.

Li, Y., and S. Yang. 2021. "Design Optimization of Metamaterial Units Using a Genetic Algorithm Based Optimization Methodology." *COMPEL: The International Journal for Computation & Mathematics in Electrical & Electronic Engineering* 40 (1): 18–26.

Manikandan, K., A. Sivabalan, R. Sundar, and P. Surya. 2020. "A Study of Landsman, Sepic and Zeta Converter by Particle Swarm Optimization Technique." In *2020 6th International Conference on Advanced Computing and Communication Systems, ICACCS 2020*, 1035–8.

Markkassery, S., A. Saradagi, A. D. Mahindrakar, S. Member, N. Lakshminarasamma, and R. Pasumarthy. 2020. "Modeling , Design and Control of Non-isolated Zeta – Buck – Boost Converter." *IEEE Transactions on Industry Applications* 56 (4): 3904–18.

Mohanty, S. N., and R. Satapathy. 2009. "An Evolutionary Multtobjecttve Genetic Algorithm to Solve 0/1 Knapsack Problem." In *Proceedings – 2009 2nd IEEE International Conference on Computer Science and Information Technology, ICCSIT 2009*, 397–9.

Murataliyev, M., M. Degano, M. D. Nardo, N. Bianchi, A. Tessarolo, W. Jara, M. Galea, and C. Gerada. 2021. "Homothetic Design in Synchronous Reluctance Machines and Effects on Torque Ripple." *IEEE Transactions on Energy Conversion* 36 (3): 2195–205.

Najdoska, A., and G. V. Cvetkovski. 2022. "Determination of Maximum Power Point from Photovoltaic System Using Genetic Algorithm." *COMPEL: The International Journal for Computation & Mathematics in Electrical & Electronic Engineering* 41 (4): 1107–19.

Priyadarshi, N., M. S. Bhaskar, P. Sanjeevikumar, F. Azam, and B. Khan. 2022. "High-Power DC–DC Converter with Proposed HSFNA MPPT for Photovoltaic Based Ultra-fast Charging System of Electric Vehicles." *IET Renewable Power Generation* 1–13, https://doi.org/10.1049/rpg2.12513.

Ragul, R., N. Shanmugasundaram, and R. Krishnakumar. 2022. "PV System with Zeta Converter Using ANFIS Controller Based GWO Optimization." In *Proceedings of the International Conference on Electronics and Renewable Systems, ICEARS 2022*, 366–70.

Rezvanyvardom, M., and A. Mirzaei. 2021. "Zero-Voltage Transition Nonisolated Bidirectional Buck-Boost DC–DC Converter with Coupled Inductors." *IEEE Journal of Emerging and Selected Topics in Power Electronics* 9 (3): 3266–75.

Sarkawi, H., Y. Ohta, and P. Rapisarda. 2021. "On the Switching Control of the DC–DC Zeta Converter Operating in Continuous Conduction Mode." *IET Control Theory and Applications* 15 (9): 1185–98.

Sayed, S. S., and A. M. Massoud. 2022. "Review on State-Of-The-Art Unidirectional Non-isolated Power Factor Correction Converters for Short-/Long-Distance Electric Vehicles." *IEEE Access* 10: 11308–40.

Wu, T., S. Member, S. Ljang, S. Member, Y. Chen, and N. Chung. 2003. "Design Optimization for M M Etr Ca I I ZVS-PVV M Rte R." 39 (2).

Wang, L., and M. Shan. 2022. "A Novel Single-Stage Common-Ground Zeta-Based Inverter with Nonelectrolytic Capacitor." *IEEE Transactions on Power Electronics* 37 (9): 11319–31.

Xiao, S., M. Rotaru, and J. K. Sykulski. 2012. "Exploration versus Exploitation Using Kriging Surrogate Modelling in Electromagnetic Design." *COMPEL – The International Journal for Computation and Mathematics in Electrical and Electronic Engineering* 31 (5): 1541–51.

Xu, B., Z. Yan, W. Zhou, L. Zhang, H. Yang, Y. Liu, and L. Liu. 2022. "A Bidirectional Integrated Equalizer Based on the Sepic–Zeta Converter for Hybrid Energy Storage System." *IEEE Transactions on Power Electronics* 37 (10): 12659–68.

Zhu, B., G. Liu, Y. Zhang, Y. Huang, and S. Hu. 2021. "Single-Switch High Step-Up Zeta Converter Based on Coat Circuit." *IEEE Access* 9: 5166–76.

Zamanan, N., J. Sykulski, and A. K. Al-Othman. 2007. "Arcing High Impedance Fault Detection Using Real Coded Genetic Algorithm." In *Proceedings of the 3rd IASTED Asian Conference on Power and Energy Systems, AsiaPES 2007*, 35–9.